Stiff, Strong, Zero Thermal Expansion Lattices via Material Hierarchy

Jeremy Lehman[1] and Roderic Lakes[2*]

1 Engineering Mechanics Program;
2 Department of Engineering Physics, Materials Science Department and Rheology Research Center,
University of Wisconsin-Madison
212 Engineering Research Building,
1500 Engineering Drive, Madison, WI 53706-1687
* address correspondence to RL: e-mail- lakes@engr.wisc.edu

adapted from
Lehman, J. J. and Lakes, R. S., "Stiff, strong, zero thermal expansion lattices via material hierarchy", Composite Structures 107, 654-663 (2014).

Abstract

For engineering applications where tight dimensional tolerances are required, or for applications where materials are subjected to a wide range of temperatures it becomes desirable to reduce a material's coefficient of thermal expansion. By carefully designing lattice microstructures, zero thermal expansion can be achieved. This work describes lattice microstructures that achieve zero expansion by utilizing either the Poisson effect to negate thermal expansion, or a curved, bi-material rib morphology. Previously described microstructures were composed of solid material constituents. The lattices presented here have structural hierarchy in which lattice ribs contain oriented porosity. This gives rise to improved strength and modulus, and provides additional design freedom associated with anisotropy.

Keywords
Zero thermal expansion
Hierarchical lattice structure
Mechanical properties
Stiffness optimization

Introduction

Low or even zero thermal expansion coefficients are desirable for materials requiring precise dimensional tolerance or subjected to environments with large temperature fluctuations. It is possible to achieve thermal expansion that is large positive, zero, or large negative by lattices with curved bi-material ribs [1, 2]. Zero expansion lattices based on this concept have been designed [3] with improved ratio of stiffness to density [4]. Lattices containing straight ribs can in principle be fully stretch-dominated and have an optimally high ratio of stiffness to density. Two-dimensional lattices with two kinds of ribs and rotating joints were introduced by Steeves et al. [5]. Zero expansion lattices constructed of curved, hexagonal honeycomb cells, with inserts consisting of three spars, made of a second dissimilar material are described by Jefferson et al [6]. Two-dimensional and three-dimensional lattices containing nested tubes were analyzed by Lehman and Lakes [7].

The nested tube morphology consists of ribs that consist of two tubes with differing coefficients of thermal expansion (CTEs) oriented concentrically, following the structural strut design of Baird [7, 8]. Zero expansion is achieved via nested tubes as follows. The difference in material thermal expansion creates a thermal stress which acts to stretch the lower CTE material circumferentially, for an increase in temperature. This circumferential extension in turn leads to a Poisson contraction in the axial direction. By carefully choosing material properties and volume ratios it is possible to fully compensate for the thermal expansion in the axial direction to achieve zero expansion. For a decrease in temperature the reverse is true, a circumferential constriction results in an axial extension negating axial thermal contraction. Two configurations exist, with the same analysis and principles applicable to both. The first configuration is to have the smaller CTE material press fitted over the larger expansion material. This ensures that the two materials remain in contact as the temperature increases. Material separation may occur for sufficiently large temperature decreases. Another configuration would be to press fit the larger CTE material over the smaller expansion material, ensuring contact for all temperature decreases, with possible material separation for sufficiently large temperature increases.

Prior analysis of lattices based on nested tubes considered both isotropic and anisotropic materials as well as two material boundary conditions [7]. The first boundary condition assumes that the constituent materials are perfectly bonded, whereas the second boundary condition assumes perfect slip condition. Previously described material structures could only achieve zero thermal expansion with the use of either the perfect slip assumption or the use of a negative CTE material. Both of these restrictions entail limited applicability. Most commonly used materials have positive thermal expansions, and the perfect slip assumption is an ideal condition. One may approximate such a condition by segmenting the larger CTE material into rings, or a wrapping of helical wire [9].

The present analysis describes zero expansion morphologies composed of positive CTE materials. Strength and stiffness of these lattices are enhanced by structural hierarchy. Structural hierarchy refers to structure within structure. Honeycombs and foams with structural hierarchy can be designed with compressive strength to density ratio orders of magnitude greater than values for conventional structures [10]. The present zero-expansion lattices are designed using ribs that themselves have oriented porosity. Lattices are considered based on nested hierarchical tubular ribs as well as lattices based on curved bi-material ribs.

Material Properties

Several materials were considered throughout this analysis. Four isotropic metals were chosen including Invar, aluminum, steel, and brass. These materials were selected for their

commonality and typical use as structural materials. Invar is well known for its small coefficient of thermal expansion. Additionally two anisotropic, unidirectional fiber composites were also considered, a graphite fiber epoxy composite and a Kevlar fiber epoxy composite. The fibers are aligned in the longitudinal direction with respect to the matrix, while the transverse direction is considered to be orthogonal to the axis of the fibers. The material properties used for each material are shown in Table 1 in which E is Young's modulus, ν is Poisson's ratio, and α is thermal expansion. The properties used are obtained as follows. The properties of Invar were obtained from Woolger [11]; the properties for Kevlar epoxy and graphite epoxy composites are from Agarwal and Broutman [12] The thermal properties for aluminum and steel are obtained from the ASM International Materials Properties Database Committee [13], while the mechanical properties of aluminum and steel are from Cook and Young [14]. The properties of Brass are those of yellow brass and were obtained from Beer et al. [15].

Table 1 provides a list of material properties used throughout the analysis. For fiber reinforced composites the *L* subscript indicates the direction along the fibers while *T* denotes transverse to the direction of the fibers. Steel, brass, aluminum, and Invar are considered isotropic and are only defined by one Young's modulus and one CTE.

Material Property	Steel	Brass	Aluminum	Invar	Unidirectional Graphite Fiber Epoxy Composite	Unidirectional Kevlar Fiber Epoxy Composite
E_L (GPa)	200	105	70	140	159	83
E_T (GPa)	--	--	--	--	10.9	5.6
ν_{LT}	0.3	0.35	0.33	0.28	0.38	0.34
α_L (μstrain/K)	12	20.9	22.2	1	0.045	-3.3
α_T (μstrain/K)	--	--	--	--	20.2	35

Zero Expansion via Oriented Porosity and the Poisson Effect

Hierarchical tubular rib based lattices contain a tube with oriented porosity along its axis. This tube is then incased by a second material which has porosity oriented circumferentially. The porosity can be distributed randomly or periodically, but it is assumed to be homogeneously distributed within the material. Figure 1 depicts this zero expansion morphology. A no slip boundary condition is assumed.

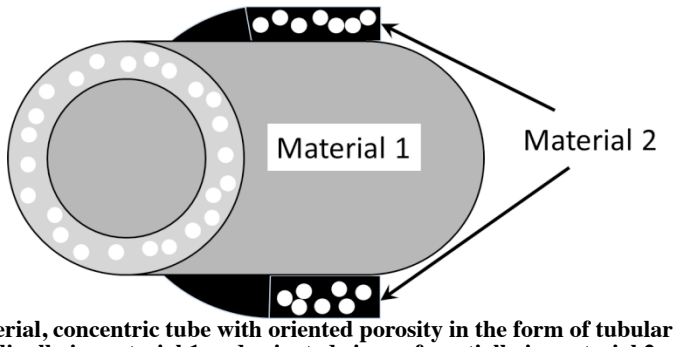

Figure 1 shows the bi-material, concentric tube with oriented porosity in the form of tubular channels oriented longitudinally in material 1 and oriented circumferentially in material 2.

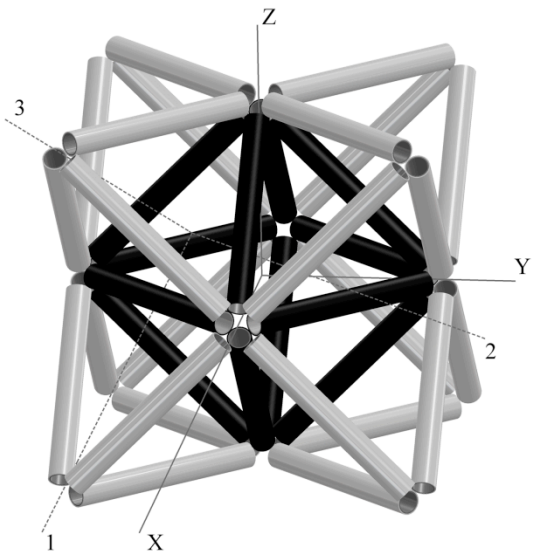

Figure 2 depicts an octet-truss lattice structure composed of nested tube rib elements. All elements are identical. The inner octahedron elements are shown in black while the exterior tetrahedral elements are depicted in white for visual clarity.

Oriented porosity in the lattice rib gives rise to tunable anisotropy of the rib material, a useful design variable, and also enhances the ratio of strength to weight. Anisotropy is achieved with the addition of oriented cylindrical pores.

The structural hierarchy can alter the mode of failure, resulting in improved strength. Both plastic yield and Euler buckling modes are considered for octet-truss lattices of zero expansion tubes. Deshpande et al. describe the octet-truss and its mechanical properties [16]. An octet-truss lattice made of nested tube elements is shown by Figure 2 [7].

The material Young's modulus along the axis of the pores is proportional to the material density, whereas in the transverse direction the elastic modulus is proportional to the relative density to the third power [17]. This difference is due to the mode of deformation for each direction. Along the axial direction the solid material's deformation is stretch dominated, but in the transverse direction, the deformation is primarily bending dominated [17]. By changing the relative density of each constituent material, the degree of anisotropy can be adjusted. Equations 1 and 2 explicitly state the Young's moduli along the axial and transverse directions.

$$E_A = C_1 \frac{\rho}{\rho_S} E_S \quad \textbf{1}$$

$$E_T = C_2 \left(\frac{\rho}{\rho_S}\right)^3 E_S \quad \textbf{2}$$

The subscript *s* indicates the material property (density or elastic modulus) corresponding that of the solid material (density or elastic modulus). The constants of proportionality (C_1 or C_2) depend on the geometry of the pores. Because the pores are perfectly aligned in the axial direction the constant C_1 is simply equal to one. The tangential constant of proportionality is somewhat more difficult to characterize, and depends upon the pore geometry. For this analysis a value of 0.8 was used for C_2. This value is equivalent to that of wood in the radial direction, as reported by Gibson and Ashby [17]. This constant is valid for wood-like relative densities, 0.05-0.8 [17], and is applicable for the range of constituent relative densities considered here.

Thermal Expansion of Nested Tubes

The total thermal expansion of the combined structure can be calculated using the relationship derived by Lehman and Lakes for thin walled bi-material tubes with a no-slip material interface [7]. The assumptions inherent to this relationship include a thin wall assumption. This implies that the radii of the two materials much greater than the wall thickness, and thus the thickness ratio ($d = t_1/t_2$) is equivalent to the volume ratio of material one to material two. Stress in the radial direction is assumed to be zero. As specified by the no slip assumption, the strain of material one is equal to the strain of material two. Equation 3 provides the expression for the total structural thermal expansion.

$$\alpha_{Sum} = \alpha_{L1} + \frac{\nu_{CL1}(\alpha_{C1}-\alpha_{C2})}{(1+n_C d)} + \left[1 - \frac{\nu_{LC1}(\nu_{CL1}+\nu_{CL2}n_C d)}{1+n_C d}\right]\left[\frac{(\alpha_{L2}-\alpha_{L1})(1+n_C d)+\frac{E_{C1}}{E_{L1}}(\alpha_{C2}-\alpha_{C1})(\nu_{LC1}+\nu_{LC2}n_L d)}{(1+n_L d)(1+n_C d)-(\nu_{LC1}+\nu_{LC2}n_L d)(\nu_{CL1}+\nu_{CL2}n_C d)}\right] \quad \mathbf{3}$$

The *L* subscript indicates the axial or longitudinal direction of the tube element, while the *C* subscript describes the circumferential direction. Material one and two are designated by their numeric subscripts. The variable *n* is a material modulus ratio, E_1 over E_2, and one ratio exists for each direction, longitudinal and circumferential. The Poisson ratios are defined by the strain ratio given by Equation 4, whereas the two Poisson ratios for each material are related as in Equation 5 [12].

$$\nu_{LC} = -\frac{\epsilon_C}{\epsilon_L} \quad \mathbf{4}$$

$$\frac{\nu_{CL}}{E_C} = \frac{\nu_{LC}}{E_L} \quad \mathbf{5}$$

By using Equations 1 through 5, aligning the pore axial direction of material one with the longitudinal direction of the tube structure, aligning the pore axial direction of material two with the circumferential direction of the tube structure, and varying both materials' relative densities for a given thickness ratio, it is possible to characterize a structure that has zero over all expansion. Zero expansion is analytically achieved for tube elements with Invar for material one and aluminum, brass or steel for material two. The contour plots shown in Figures 3-5 represent zero expansion tube elements. Each contour represents a different thickness ratio ($d = t_1/t_2$), and is labeled with this value. The plot axes indicate the material relative densities.

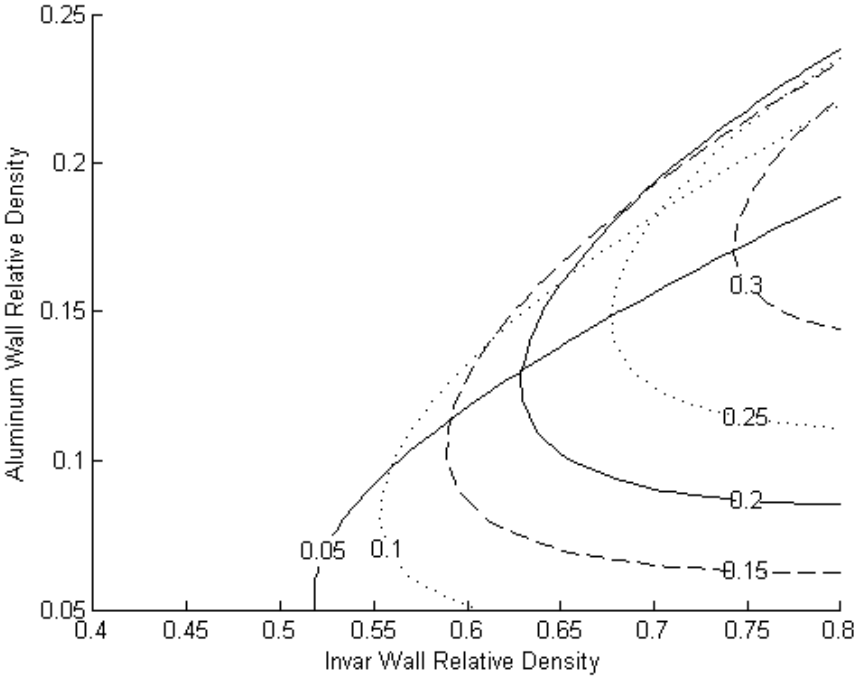

Figure 3 plots contours of zero expansion for different geometry values for hierarchical tubular lattices. Material one is Invar; material two is aluminum. Contour labels represent thickness ratio $d = t_1/t_2$.

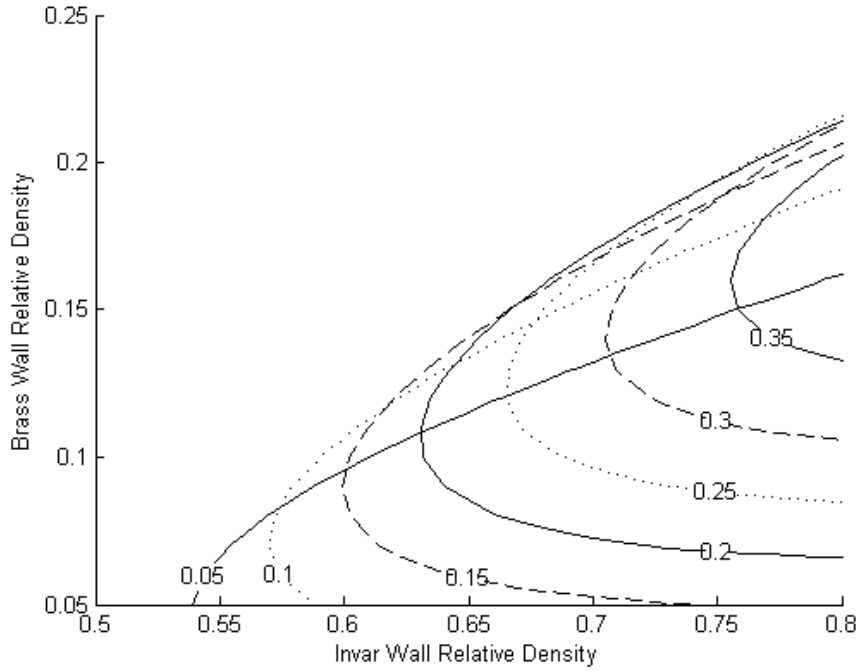

Figure 4 plots contours of zero expansion for different geometry values for hierarchical tubular lattices. Material one is Invar; material two is brass. Contour labels represent thickness ratio $d = t_1/t_2$.

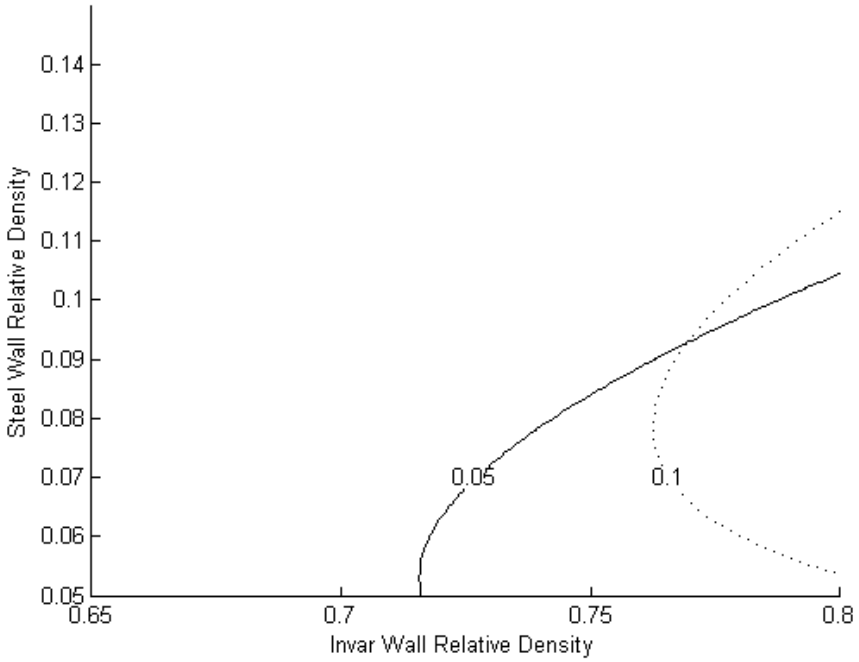

Figure 5 plots contours of zero expansion for different geometry values for hierarchical tubular lattices. Material one is Invar; material two is steel. Contour labels represent thickness ratio $d = t_1/t_2$.

From a design and manufacturing perspective, it is simpler if only one of the materials contains oriented porosity. Indeed, for all three material combinations shown, zero expansion can be achieved in which material one, Invar, is fully dense without porosity. In that case, not plotted in Figures 3-5, an optimal thickness ratio exists, maximizing the relative density of material two. For Invar and aluminum, a thickness ratio of 0.2 allows for zero expansion with an aluminum relative density as much as 0.33. For steel and Invar a thickness ratio of 0.25 and a steel relative density of 0.24 can achieve zero expansion.

Parametric Study

It has been shown that zero thermal expansion is attainable with Invar paired with aluminum, brass, or steel. It is desirable to gain insight into which other material combinations are capable of obtaining zero expansion. To achieve further insight a parametric study was conducted where various parameters are held constant while others are allowed to vary, in order to see which geometries and material properties can achieve zero expansion.

Equation 3 is rewritten for the specific case where two initially isotropic materials are considered to have equal Poisson's ratios. It is then possible to write the total overall expansion in terms of the relative density of material 1 ($\bar{\rho}_1$), the relative density of material two ($\bar{\rho}_2$), the thermal expansion ratio of material two to material one, Poisson's ratio (ν), the effective stiffness ratio of material one to material two (nd) with the modulus ratio given by $n = E_1/E_2$ and the constant of proportionality (C_2) of Equation 2. The effective stiffness ratio is defined as the Young's modulus of material one times the thickness of material one, divided by the product of the thickness and modulus of material two. The porosity is assumed to be oriented as shown in Figure 1, and to run the full length of the material. This geometry implies that the constant of proportionality in the axial direction (C_1) is one, while C_2 is again considered to be 0.8 after the wood model provided by Gibson and Ashby [17]. By constraining the overall thermal expansion to be zero and varying the effective stiffness and relative density of material two while holding all parameters constant it is possible to compute the ratio of material thermal expansions required

to achieve zero thermal expansion. Equation 6 provides the relationship for overall thermal expansion which was used to complete the parametric study.

$$\alpha_{Sum} = \alpha_1 \left(1 + \left(\frac{\nu C_2 \rho_1^{\bar{2}}}{1 + C_2 \frac{\theta_1^{\bar{2}}}{\theta_2} nd} \right) \left(1 - \frac{\alpha_2}{\alpha_1} \right) + \left(\frac{\alpha_2}{\alpha_1} - 1 \right) \left(1 - \frac{\nu^2 \left(1 + C_2^{\bar{2}} \rho_2 \rho_1^{\bar{2}} nd \right)}{1 + C_2 \frac{\theta_1^{\bar{2}}}{\theta_2} nd} \right) \frac{\left(1 + C_2 \frac{\theta_1^{\bar{2}}}{\theta_2} nd + \nu \rho_1^{\bar{2}} C_2 \left(1 + \frac{\theta_2}{\theta_2} nd \right) \right)}{\left(1 + C_2 \frac{\theta_1^{\bar{2}}}{\theta_2} nd \right) \left(1 + \frac{\theta_2}{C_2 \theta_2^{\bar{2}}} nd \right) - \nu^2 \rho_1^{\bar{2}} C_2 \left(1 + \frac{\theta_2}{\theta_2} nd \right)^2} \right) \quad \mathbf{6}$$

Using three different values for the relative density of material one and varying material two relative density, Figures 6-8 are generated. Figure 6 provides

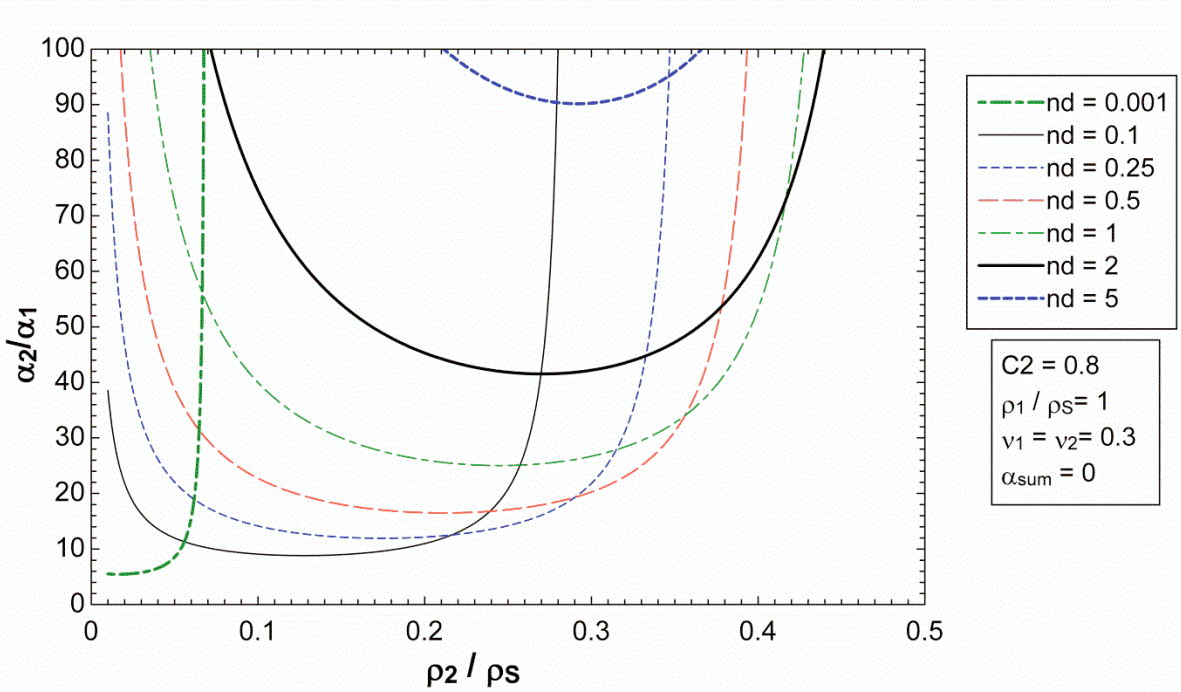

Figure 6 indicates the required ratio of thermal expansion coefficients required to achieve zero overall thermal expansion for nested tubes with a material one relative density of 1.0, Poisson's ratios equal to 0.3 and varying effective stiffness ratios and material two relative densities. *nd* = E_1t_1/E_2t_2 is the ratio of structural stiffness of the two tube materials.

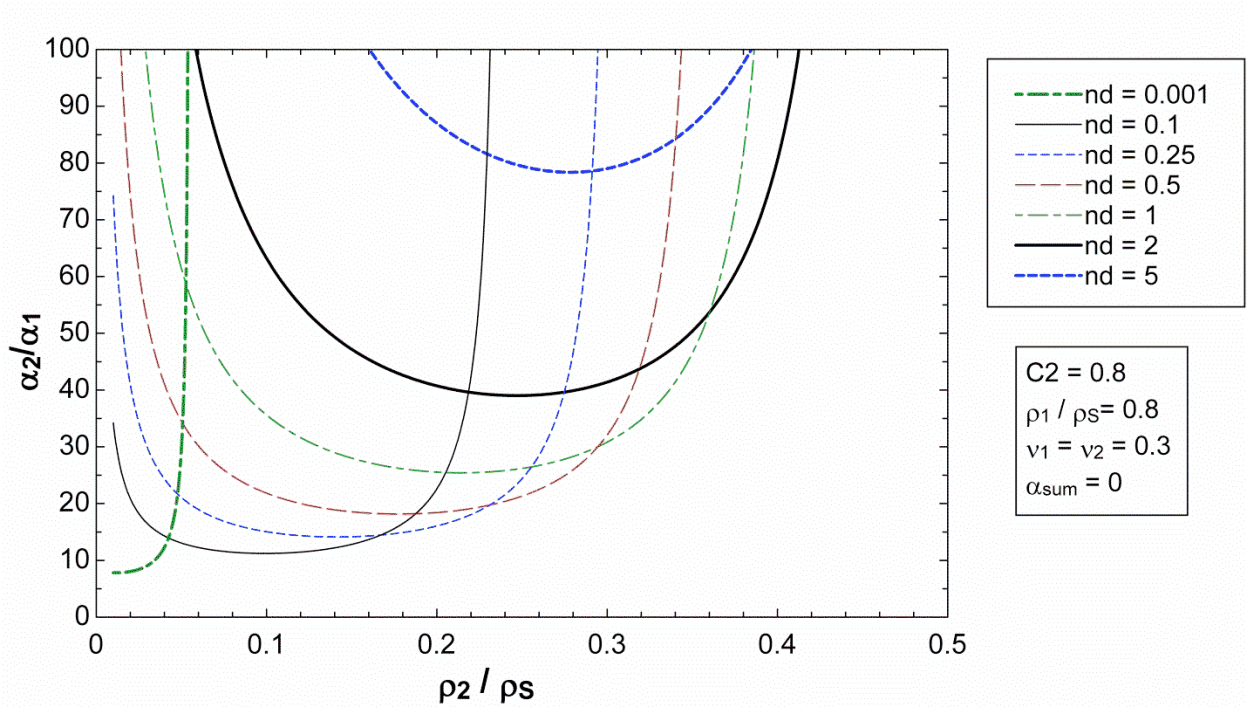

Figure 7 indicates the required ratio of thermal expansion coefficients required to achieve zero overall thermal expansion for nested tubes with a material one relative density of 0.8, Poisson's ratios equal to 0.3 and varying effective stiffness ratios and material two relative densities. *nd* = E_1t_1/E_2t_2 is the ratio of structural stiffness of the two tube materials.

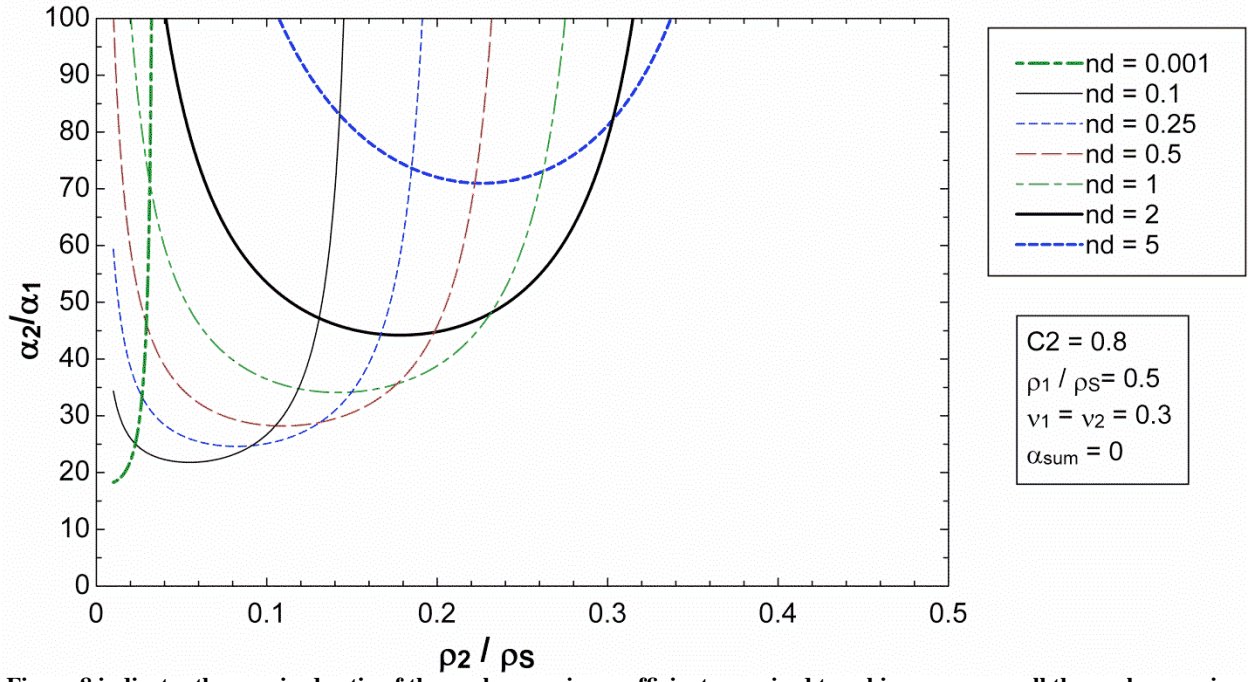

Figure 8 indicates the required ratio of thermal expansion coefficients required to achieve zero overall thermal expansion for nested tubes with a material one relative density of 0.5, Poisson's ratios equal to 0.3 and varying effective stiffness ratios and material two relative densities. *nd* = E_1t_1/E_2t_2 is the ratio of structural stiffness of the two tube materials.

From Figures 6-8 it is possible to make inferences about what material combinations can possibly achieve zero thermal expansion. By selecting an effective stiffness ratio and determining from the plots the minimum required ratio of thermal expansion ratio, one can determine if two materials can be used to make a tubular lattice with zero expansion. It is desirable to consider materials with a small expansion ratio α_1/α_2 to expand the design space. Moreover, an ideal material combination would have a material one with a small Young's modulus and small thermal expansion in comparison to material two. For most materials these properties are contradictory. Most materials with low thermal expansion are also quite stiff, while high expansion materials are considerably less stiff. Invar is unique in that it has a very small expansion and is still quite stiff. The thermal expansion ratio for steel to Invar is 12, while for aluminum and Invar it is 22.2. Many polymers when paired with other polymers have expansion ratios of approximately 3-5 [18]. This difference in expansion is too small to achieve zero overall expansion with pairs of polymers. Small expansion ratios can be used provided the structural stiffness ratio $nd = E_1t_1/E_2t_2$ is high. There are practical limits on this ratio. However Figure 4 shows that for an effective stiffness ratio of 0.1 can achieve zero expansion with a material thermal expansion ratio of as little as 9. This can be achieved with Invar-steel, Invar-aluminum, and Invar-brass. Several metal-polymer combinations were considered. Of those considered, Invar and high density polyethylene (HDPE) can achieve zero expansion with a thickness ratio of 0.06. This implies a solid volume fraction of 5.7 % Invar to 94.3% HDPE.

It is also important to consider the structural properties of this morphology. A two dimensional honeycomb can be constructed of zero expansion nested tube elements. Stiffness is enhanced by organizing the tubular elements in an equilateral triangular lattice. This lattice structure has deformation that is predominantly axial to the constituent elements. A stretch as opposed to bending dominant structure has greater in plane stiffness because a stretch dominant structure's stiffness will be linearly proportional to relative density whereas a bending dominant structure will be a quadratic function of relative density [17]. The relative stiffness of a lattice structure as well as relative density serve as useful measures of a material's performance. By modifying previously derived results for triangular, tubular honeycombs [7], and allowing for oriented porosity within materials one and two, Equations 7 and 8 are obtained.

$$\frac{E_H}{E_S} = \frac{\pi}{\sqrt{3}}\rho_2 \frac{\left(d\frac{\rho_1}{\rho_2}+1\right)}{nd\frac{\rho_1}{\rho_2}+1}\left(2-\frac{t}{r}\right)\frac{t}{L}\frac{nd\frac{\rho_1}{\rho_2}+C_2\rho_2^2}{d+1} \quad \textbf{7}$$

$$\frac{\rho^*}{\rho_s} = \pi\sqrt{3}\rho_2\left(2-\frac{t}{r}\right)\frac{t}{L}\frac{d\frac{\rho_1}{\rho_2}+1}{d+1} \quad \textbf{8}$$

Adding porosity to material one actually decreases the performance of the overall zero expansion structure. This can be conceptualized by studying the relationship of Equation 5. The Poisson ratio ν_{CL1} actually decreases as porosity is added. This means that by adding porosity, more circumferential displacement is required to achieve the same longitudinal contraction. The magnitude of the Poisson effect is reduced as porosity is added to material one.

Zero Expansion via Oriented Porosity and Curved Bi-material Rib Elements

The second morphology analyzed is that of curved, bi-material rib elements with added porosity. The added porosity, oriented along the axis of the curved element, allows the sectional properties of both materials to vary, without any additional material. The area moment of inertia can be increased if the amount of material remains constant but is allowed to occupy more space. Adjusting the sectional properties of both constituent materials was considered in the context of section shape [4] and is further expanded by the analysis of elements with porosity. The result of added porosity is compared to prior honeycomb lattices via a stiffness density map.

Curved bi-material rib elements consist of two layers of differing materials fully bonded to one another. As the temperature fluctuates, a bending moment is created which will result in a slight change in curvature. By carefully selecting the material, and geometric properties including a slight initial curvature, the overall expansion of the two end points of the rib can be negated. That is, the axial expansion is counteracted by the increasing curvature of the element resulting in a zero net displacement of the end nodes. Thermal expansion of such ribs is given by Equation 9 [3]. This structural expansion represents the thermal expansion coefficient along the chord wise direction of the bi-material curved rib element. It applies to ribs with solid, rectangular cross sections. The subscripts refer to either material one or two, where material one is located on the interior of the curved element while material two is exterior. Figure 9 depicts a single curved rib element depicting materials one and two, as well as indicating the Length L_{arc} and interior angle θ.

$$\alpha_{sum} = (\alpha_1 - \alpha_2)\frac{L_{arc}}{t}\left(\frac{\theta}{2}\right)\frac{(m+1)^2}{3(m+1)^2+(mn+1)\left(m^2+\frac{1}{mn}\right)} + \frac{\alpha_1+\alpha_2}{2} + (\alpha_2 - \alpha_1)\left[\frac{4m^2+3m+\frac{1}{mn}}{nm^3+4m^2+6m+\frac{1}{mn}+4} - \frac{1}{2}\right] \quad \mathbf{9}$$

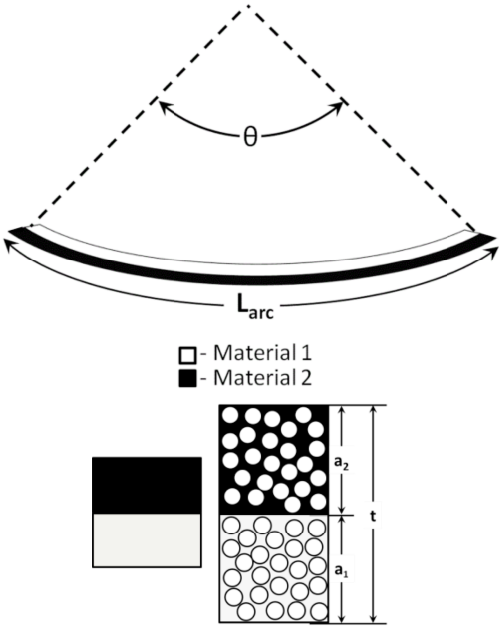

Figure 9 illustrates a single bi-material, curved rib element viewed from the out of plane direction [3], and in cross section. It indicates the arc length, materials one and two and the included angle, as well as depicting the additional porosity and thickness in cross section. The cross sectional view depicts a solid section, and a porous section. The porous section has relative densities of material one and two equal to 0.5. Each cross section has an equal amount of solid material, and equal material thickness ratios *m*.

The thickness in the plane shown by Figure 9 is *t*. The non-dimensional parameters *n* and *m* indicate the material stiffness ratio of material one to material two, and the material thickness ratio of material one to material two.

Porosity is added by specifying the relative density of material one, relative density of material two and the ratio of material one relative density to material two relative density as ρ_1, ρ_2 and *r* respectively. The porosity itself is assumed to be on a scale much smaller than that of the rib. For this reason the material is treated as a homogeneous mixture, similar to that of wood. The porosity can be distributed randomly or periodically, however heterogeneity is assumed to be sufficiently small that the porous material can be viewed as a continuum. For constant lattice

relative density if porosity is added while holding all other geometric constants equal the thickness of the cross section will increase as shown in Figure 9. This increase in cross sectional area will lead to increased bending stiffness for a particular relative density. Additionally by specifying unequal constituent relative densities (*r* not equal to one) the stiffness of one constituent can be increased relative to the other, allowing for increased bending as a result of the material thermal expansion mismatch. Increased thermal bending allows zero expansion to be achieved with a smaller initial curvature, which again enhances stiffness. This analysis assumes that the porosity is oriented along the axis of the rib, and thus the stiffness with porosity is simply proportional to the amount of void space added. The overall expansion for a rectangular section with porosity added is given by Equation 10, which is modified from the solid result.

$$\alpha_{sum} = (\alpha_1 - \alpha_2)\frac{L_{arc}}{t}\left(\frac{\theta}{2}\right)\frac{(m+1)^2}{3(m+1)^2+(mnr+1)\left(m^2+\frac{1}{mnr}\right)} + \frac{\alpha_1+\alpha_2}{2} + (\alpha_2 - \alpha_1)\left[\frac{4m^2+3m+\frac{1}{mnr}}{nm^3+4m^2+6m+\frac{1}{mnr}+4} - \frac{1}{2}\right] \quad \textbf{10}$$

The first term of Equation 10 is negative when the CTE of material one is smaller than material two, while the other two terms are positive. By carefully selecting the geometry and material pair it is possible to obtain zero or even negative values of thermal expansion for the rib element in the chord direction. By creating a two dimensional honeycomb lattice of rib elements it is possible to envisage a material that has zero net thermal expansion in two directions. This lattice is shown in Figure 10 [3].

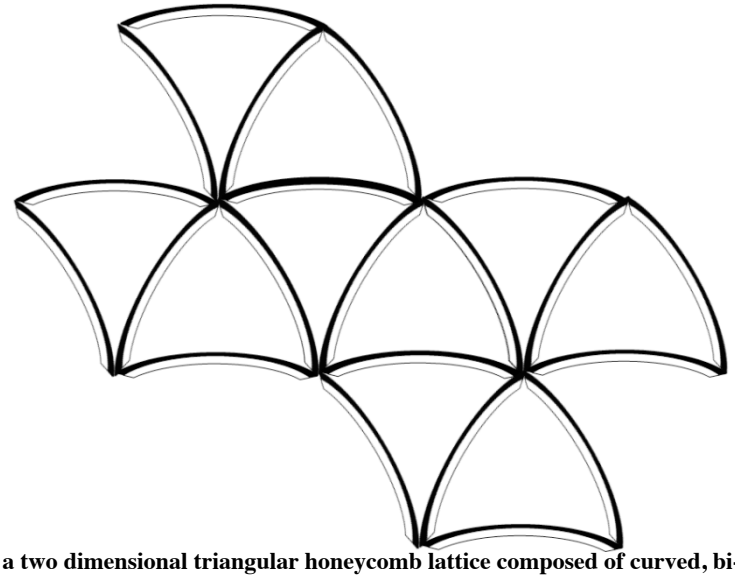

Figure 10 illustrates a two dimensional triangular honeycomb lattice composed of curved, bi-material rib elements.

By specifying an initial curvature the lattice can be tailored to achieve zero thermal expansion. This initial curvature will reduce the lattice in plane stiffness because of the added bending deformation. For this reason it is necessary to describe the overall in plane lattice stiffness as a function of material and geometric parameters. Similarly to accounting for porosity in the thermal expansion coefficient, the honeycomb stiffness can be modified from the results for solid ribs. Again, the stiffness ratio *n* is modified by a factor *r*, additionally because a continuum approach is used, the stiffness of material two is replaced with the stiffness of material two times the relative density of material 2. Equation 11 provides a formula for the overall stiffness of the honeycomb in plane.

$$E_H = \frac{4}{\sqrt{3}}\left(\frac{t}{L_{arc}}\right)\frac{E_2\rho_2(mnr+1)}{m+1}\left[\frac{\theta^3}{24\left(\frac{L_{arc}}{t}\right)^2\left(\frac{\theta}{2}cos(\theta)+\theta-\frac{3}{2}sin(\theta)\right)+3\theta^2 sin(\theta)-\theta^3}\right] \quad \textbf{11}$$

A useful dimensionless parameter for comparing the performance of this lattice to others is to normalize the stiffness by the solid material stiffness. In this case the solid stiffness is simply a weighted average of the solid volume of material one to the solid volume of material two. Equations 12 and 13 provide both the solid stiffness and the relative stiffness for the present lattice.

$$E_S = \frac{E_2\rho_2(mnr+1)}{m+1} \quad \textbf{12}$$

$$E_H/E_s = \frac{4}{\sqrt{3}}\left(\frac{t}{L_{arc}}\right)\frac{\rho_2(mr+1)}{m+1}\left[\frac{\theta^3}{24\left(\frac{L_{arc}}{t}\right)^2\left(\frac{\theta}{2}cos(\theta)+\theta-\frac{3}{2}sin(\theta)\right)+3\theta^2 sin(\theta)-\theta^3}\right] \quad \textbf{13}$$

It is necessary to determine the lattice overall relative density in order to make a side by side comparison to prior lattice structures. The relative density is obtained by modifying the previous results for a solid lattice structure, but then multiplying by al factor accounting for the porosity within each individual rib element. Equation 14 provides the relative density of the overall lattice structure with added porosity.

$$\frac{\rho^*}{\rho_S} = \frac{\sqrt{3}}{2}\left(\frac{\theta^2}{\sin^2\left(\frac{\theta}{2}\right)}\right)\left(\frac{\rho_2(mr+1)}{m+1}\right)\left(\frac{t}{L_{arc}}\right) \quad \textbf{14}$$

The ratio of relative stiffness to relative density for both solid and porous lattices is the same. There is however an advantage to adding porosity because of its effect on thermal expansion. By increasing the geometric stiffness of material one relative to material two, a rib with less initial curvature can be used to attain zero expansion. This in turn leads to a stiffer lattice configuration. Figures 11 and 12 plot relative stiffness versus relative density, where material one is Invar and material two steel. Figure 11 holds the relative density of material one constant while material two's relative density is varied. Additionally dashed lines are plotted that represent solid non-zero expansion lattices. The equilateral triangular lattice is dominated by axial deformation and thus can be considered to be optimally stiff. The regular hexagonal honeycomb primarily undergoes bending deformation, and is less stiff as a result. Figure 12 varies the relative density of material one, while holding material two's relative density constant.

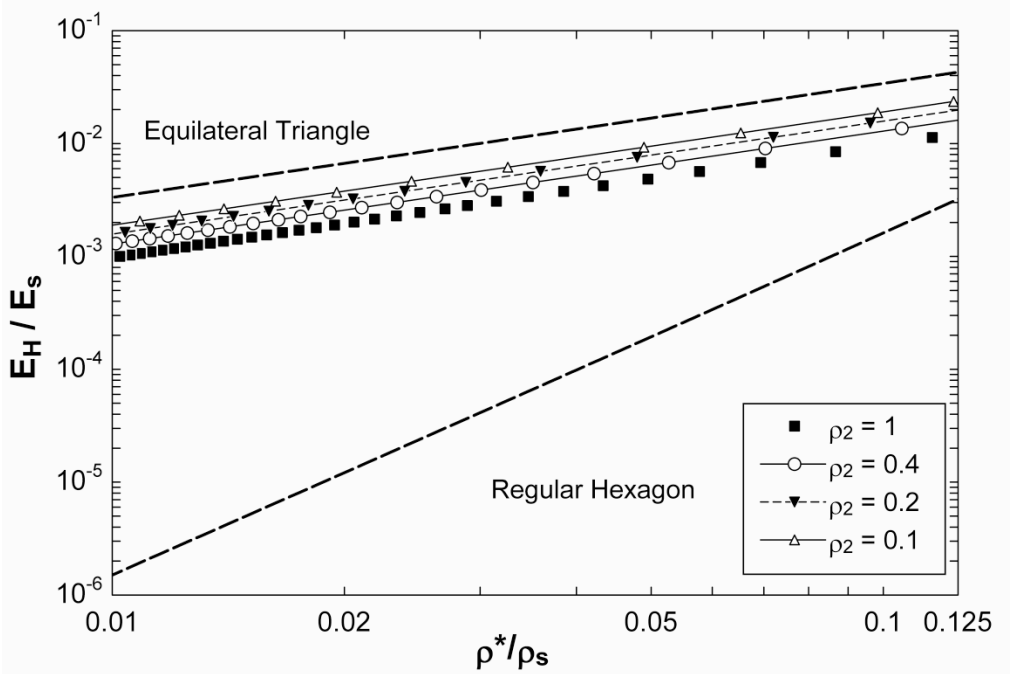

Figure 11 plots relative stiffness versus relative density for a porous, curved, bi-material, triangular honeycomb. The relative density of material one, Invar, is constant and equal to one, while the relative density of material 2, steel, is varied. The dashed lines represent non-zero expansion lattices representing equilateral and regular hexagonal honeycombs.

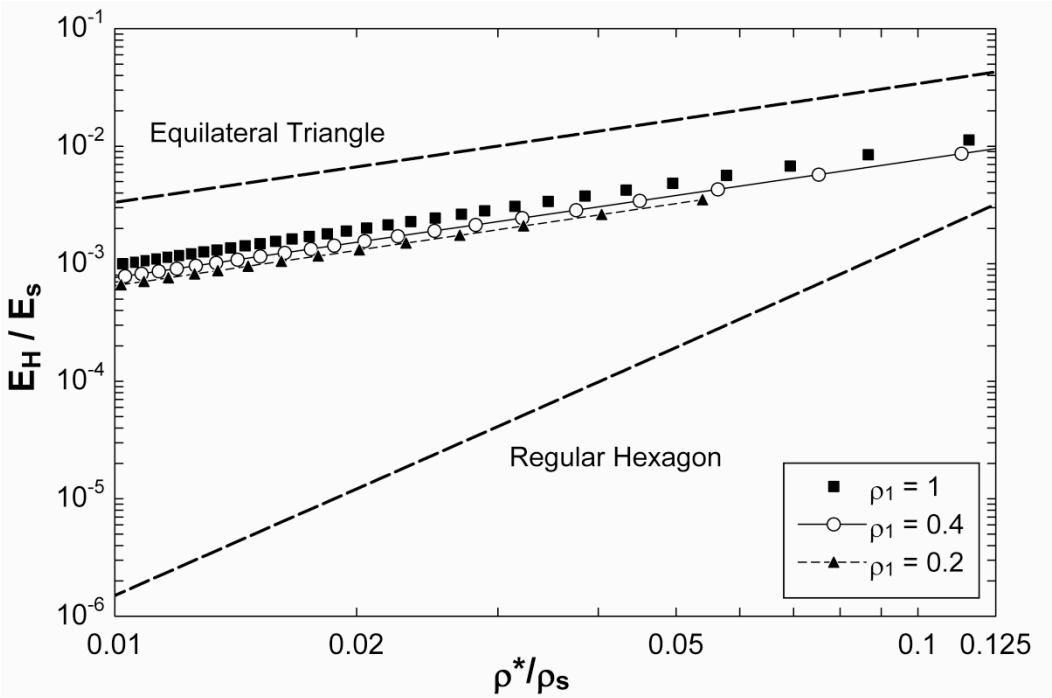

Figure 12 plots relative stiffness versus relative density for a porous, curved, bi-material, triangular honeycomb. The relative density of material two, steel, is constant and equal to one, while the relative density of material one, Invar, is varied. The dashed lines represent non-zero expansion lattices representing equilateral and regular hexagonal honeycombs.

Figure 11 indicates that as the relative density of material two is decreased, the relative stiffness ratio is improved for a given relative density. The opposite is true when the relative density of material one is decreased as shown by Figure 12. This can be explained by the fact that as you add porosity to material two, the stiffness of material one relative to that of two is increased. Because material one is the smaller CTE constituent, increasing its stiffness will create a large bending moment due to a change in temperature. This allows for zero overall expansion with a smaller initial curvature then a rib element with no added porosity. With less curvature, the penalty in stiffness is decreased. So it is better to add oriented porosity to the material with higher expansion because that leads to a stiffer lattice.

The present porous rib elements are compared with previously described rib elements with Tee shaped cross sections. Figure 13 plots relative densities versus relative stiffness of both the porous honeycombs of Figure 11 and two different Tee shaped cross section. Each Tee shaped cross section is described by the dimensionless parameter *j*, or the ratio of the width of material one to the width of material two, where width indicates the out of plane direction of the honeycomb. The two section geometries included here are *j* equal to 5 and *j* equal to 20. This shows that ribs based on structural hierarchy provide stiffness enhancement comparable to engineered shaping of the rib cross section.

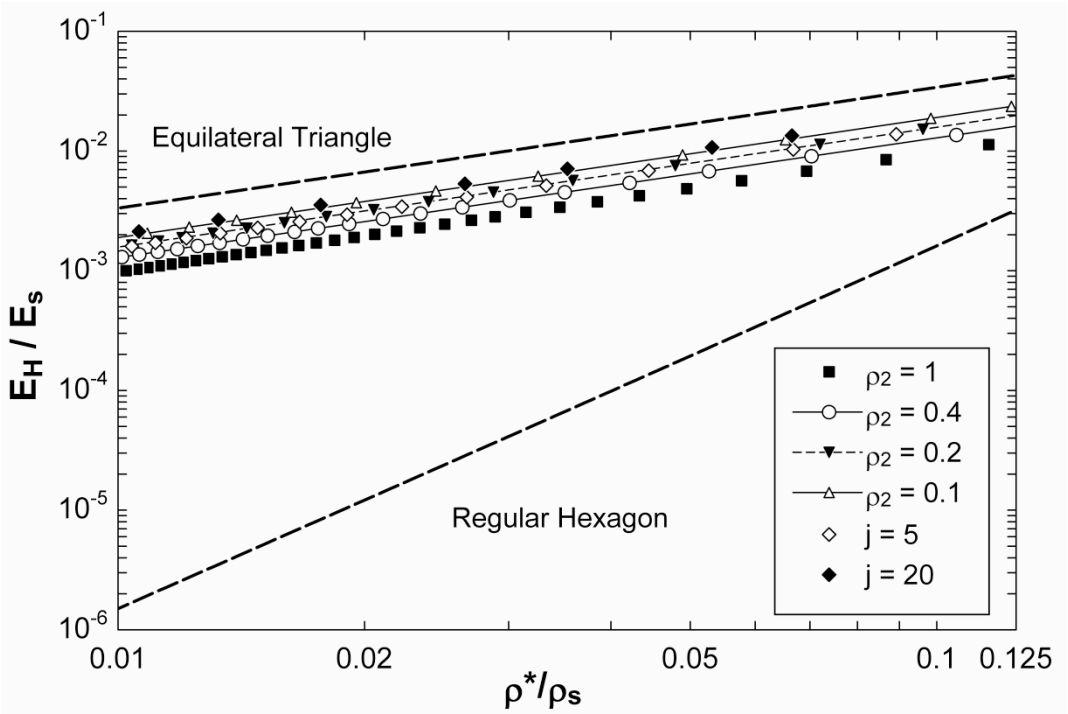

Figure 13 plots relative stiffness versus relative density for both porous, curved, bi-material, triangular honeycombs and curved, bi-material, triangular honeycombs with Tee shaped cross sections. For the porous lattices the relative density of material one, Invar, is constant and equal to one, while the relative density of material two, steel, is varied. Tee shaped lattices where *j* = 5 and *j* = 20 are shown. The dashed lines represent non-zero expansion lattices representing equilateral and regular hexagonal honeycombs.

An additional comparison can be made with tubular lattices previously studied. The tubular lattices described by Lehman and Lakes [4] are composed of solid, non-porous constituents but approximate a perfect slip interface by using a wire wrapped morphology. The second material is considered to be helical band or wire nested over the thin walled tube of material one. This allows material two to participate in applying circumferential stress to the other tube, while decreasing its axial contribution. Figure 14 plots in addition to curved porous ribs of zero expansion with varying material two relative density two wire wrapped tube zero

expansion morphologies. The first tubular morphology is that of an Invar tube wrapped with aluminum wire and is plotted using open diamonds. The other tubular morphology shown is that of an Invar tube wrapped with steel wire and is indicated with solid diamonds.

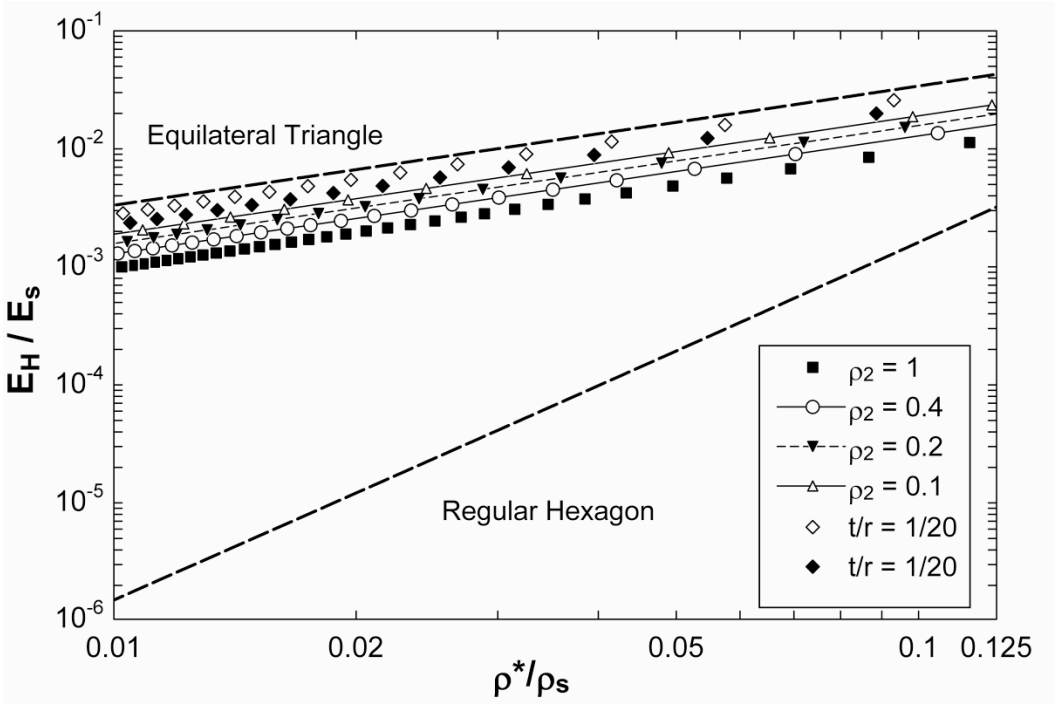

Figure 14 plots relative stiffness versus relative density for porous curved, bi-material, triangular honeycombs and wire wrapped, bi-material, tubular, triangular honeycombs. For the porous lattices the relative density of material one, Invar, is constant and equal to one, while the relative density of material two, steel, is varied. Wire wrapped tube morphologies lattices where *t/r = 20* are shown. Open diamonds indicate Invar tubes wrapped with aluminum while solid diamonds indicate Invar tubes wrapped with steel. The dashed lines represent non-zero expansion lattices representing equilateral and regular hexagonal honeycombs.

From Figure 14 it can be seen that by adding porosity to the curved bi-material lattice structure can enhance the relative stiffness performance to near that of the wire wrapped tube morphology. Although the enhanced stiffness is not as great as the tubular morphologies shown the present lattice structures benefit by utilizing a less complex geometry, and do not require the approximation of an ideal condition. These two attributes would be advantageous from a practical standpoint.

To compare both porous, curved, bi-material rib and porous nested tube morphologies the relative density of each is plotted in Figure 15.

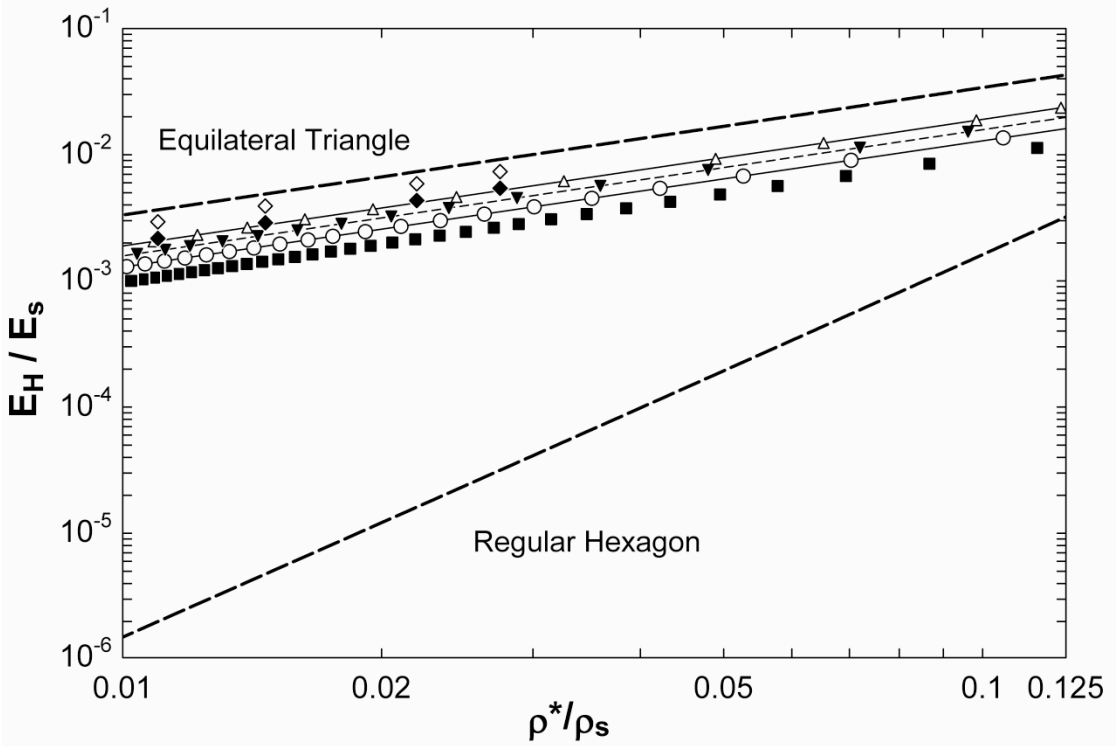

Figure 15 plots relative stiffness versus relative density for porous curved, bi-material, triangular honeycombs and wire wrapped, bi-material, tubular, triangular honeycombs. For the porous lattices the relative density of material one, Invar, is constant and equal to one, while the relative density of material two, steel, is varied. Solid squares indicate a solid cross section, open circles, closed inverted triangles, and open triangles represent material two relative densities of 0.4, 0.2, and 0.1 respectively. Nested tube morphology lattices where *t/r = 10* are shown. Open diamonds indicate solid Invar tubes wrapped with porous aluminum while solid diamonds indicate solid Invar tubes wrapped with porous steel. The relative densities of the porous materials are 0.2. The dashed lines represent non-zero expansion lattices representing equilateral and regular hexagonal honeycombs.

The strength of lattices composed of curved rib elements is also enhanced by added porosity. As an increasing load is applied, the curvature of the rib element will increase non-linearly until the element becomes structurally unstable. By increasing the area moment of inertia, the change in curvature associated with each load increment is reduced. This in turn leads to a larger load capable of being supported and thus an enhanced material strength.

Effect of Hierarchical Porosity on Strength of 3-D Zero Expansion Lattices

Oriented porosity impacts a material's thermal expansion and mechanical stiffness and can also improve the failure strength of the material. Adding porosity can alter the mode of failure. The failure mode with the smallest critical stress will determine which failure mode prevails. For low density cellular structures the elastic buckling of the material's constituent members often times is the dominant failure mode. By adding porosity, the same amount of solid material will occupy more volume, and as a result will possess a larger area moment of inertia. This increased moment of inertia leads to an increased critical buckling stress. This proves advantageous to a point where another failure mode will become the dominant failure mode.

To study how overall material strength is affected by porosity, an octet-truss three dimensional lattice structure was chosen. Each lattice member is tailored to have zero thermal expansion. The materials chosen for this analysis are Kevlar epoxy fiber composite, and Invar. The constituents are bonded together as concentric, thin-walled tubes. The Kevlar fibers are oriented along the tube axis. Because Kevlar epoxy has a negative expansion coefficient along the fiber direction, oriented porosity is not necessary to achieve zero thermal expansion, but is

helpful in improving strength. From prior equations of thermal expansion for fully bonded anisotropic materials derived by Lehman and Lakes [7], the thickness ratio of Invar to Kevlar composite required to achieve zero thermal expansion is 1.88. This translates to a material that is 65.3% Invar and 34.7% Kevlar composite.

The added porosity is oriented axially along the tube. An identical amount of porosity is added to both material constituents. The porosity is described as the wall relative density. Adding porosity to the structure will impact the constituent Poisson ratios, resulting in slightly non zero thermal expansions, unless compensated by tuning other design variables. For the purposes of studying the material strength, this effect is ignored, and the ratio of Kevlar fiber composite to Invar is held constant throughout. The solid stiffness is computed as simply the weighted average of material one's Young modulus to that of material two.

Two failure modes were considered, Euler buckling and plastic yielding. For this analysis 3 separate hierarchical orders are considered. Each order of hierarchy (n) represents a level of structural complexity. The 0^{th} order is considered to be an octet-truss lattice composed of solid rib elements. The 1^{st} order of hierarchy considered is to redistribute the cross sectional area to that of a thin walled zero expansion morphology, while adding oriented porosity to the material constituents themselves is considered to be of a hierarchical order of 2.

The formula for determining the Euler critical stress applied to the lattice structure in the Z direction has been determined previously by Despande et al. [16] for solid rod elements and Lehman and Lakes for tube elements [7]. The relative density of the octet-lattice is dependent upon three parameters: wall relative density, wall thickness to radius ratio, and the ratio of the radius to length of an element. Equation 15 is obtained by modifying the relative density of the octet-truss composed of solid rod elements [15] to account for the added void space due to both the hollow tubular center and the added wall porosity.

$$\frac{\rho^*}{\rho_s} = \rho_{wall} 6\pi\sqrt{2} \left(\frac{r}{L}\right)^2 \left(2 - \frac{t}{r}\right)\frac{t}{r} \quad \textbf{15}$$

For this comparison the cross sectional area of each element is held constant. This means that if relative density is held constant, and so too is the thickness to radius ratio, then the aspect ratio, r over L, must change according to Equation 15. This allows the stiffness of each element to remain the same for changing densities because the load carried by each element is constant and so too is the solid area. The relationship for Euler buckling resulting from an applied load in the octet-truss Z direction has previously been derived and is repeated here by Equation 16 [7].

$$\sigma_{ZZ}^* = \frac{\pi^3\left(1-\left(1-\frac{t}{r}\right)^4\right)E}{\sqrt{2}}\left(\frac{r}{L}\right)^4 \quad \textbf{16}$$

E is the solid stiffness computed as the weighted average of the two constituent materials. The second failure mode considered is that of plastic yielding. The failure criterion for plastic yielding is that described by Gibson and Ashby for wood, given by Equation 17 [17].

$$\sigma_{pl} = 0.34\sigma_{ys}\rho_{wall} \quad \textbf{17}$$

The material yield stress is taken to be a weighted average of the compressive failure stress of Kevlar fiber epoxy composite valid within a temperature range of -79 to 100 degrees Celsius, 286 MPa [12], and Invar 385 MPa [11]. By relating the force applied to each element to the macroscopic stress applied in the Z direction to the octet lattice, the plastic yield stress can be obtained. Equation 18 is used to calculate the plastic yield stress.

$$\sigma_{zz}^{*} = 2\pi\sqrt{2}\frac{t}{r}\left(2-\frac{t}{r}\right)\left(\frac{r}{L}\right)^{2}\sigma_{pl} \qquad \textbf{18}$$

Using Equations 15-18, and holding relative density and the thickness to radius ratio constant, the critical stress for each failure mode can be plotted. The relative density of Figure 16 is 10^{-4}, t/r = 1/10, and the aspect ratio is allowed to vary. Figure 17 plots the identical conditions, but with a constant relative density of 10^{-3}.

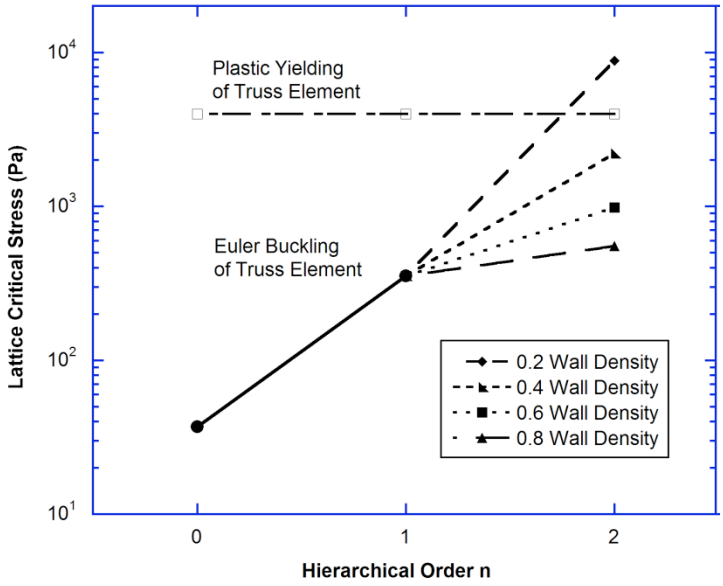

Figure 16 plots the critical stress applied to the lattice Z direction for three hierarchical orders (n). *n = 0* indicates an octet truss composed of solid rod elements, *n = 1* indicates a tubular element with solid walls, and *n = 2* indicates a tubular element with porous walls. The lattice relative density and thickness to radius ratio (for n greater than 0) are held constant and equal to 10^{-4} and 1/10 respectively.

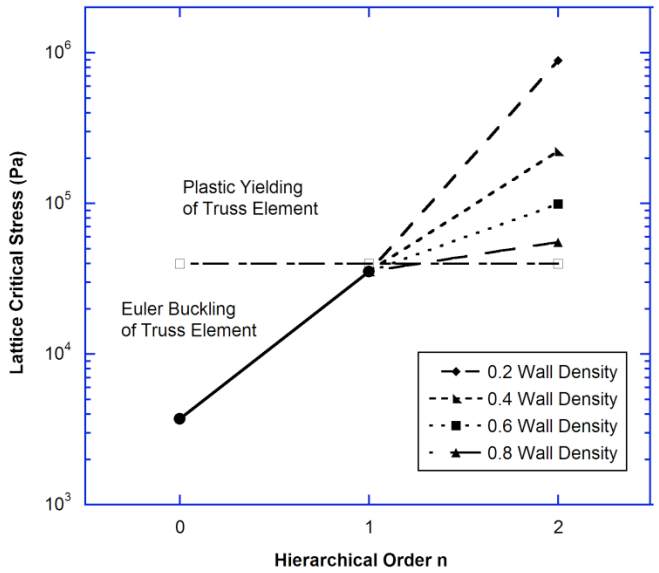

Figure 17 plots the critical stress applied to the lattice Z direction for three hierarchical orders (n). *n = 0* indicates an octet truss composed of solid rod elements, *n = 1* indicates a tubular element with solid walls, and *n = 2* indicates a tubular element with porous walls. The lattice relative density and thickness to radius ratio (for n greater than 0) are held constant and equal to 10^{-3} and 1/10 respectively.

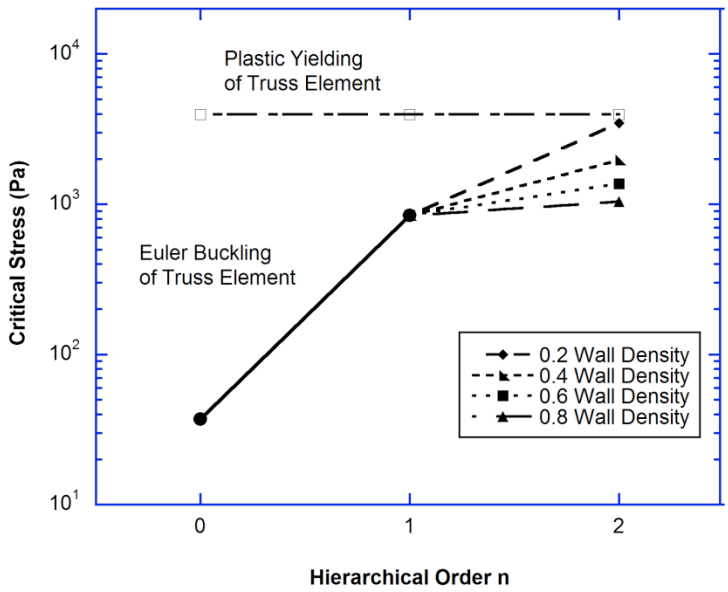

Figure 18 plots the critical stress applied to the lattice Z direction for three hierarchical orders (n). *n = 0* indicates an octet truss composed of solid rod elements, *n = 1* indicates a tubular element with solid walls, and *n = 2* indicates a tubular element with porous walls. The lattice relative density and length to radius ratio (for n greater than 0) are held constant and equal to 10^{-4} and 150 respectively.

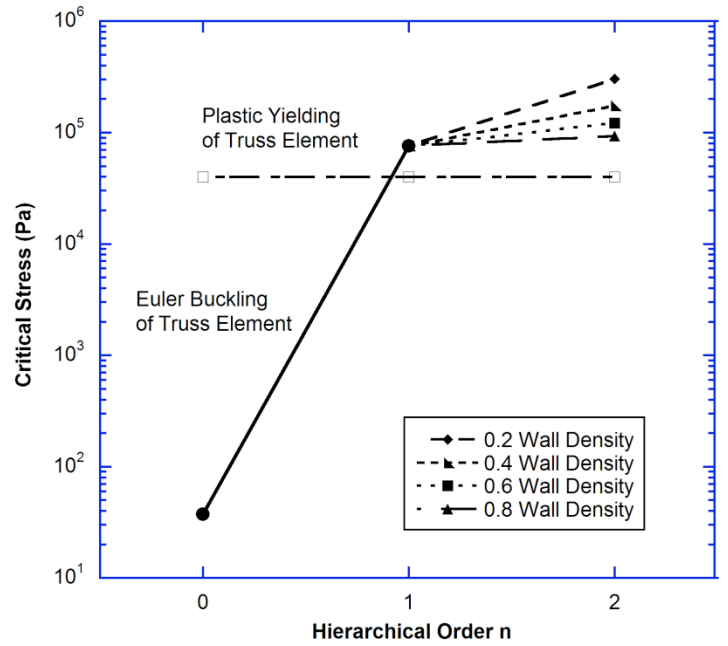

Figure 19 plots the critical stress applied to the lattice Z direction for three hierarchical orders (n). *n = 0* indicates an octet truss composed of solid rod elements, *n = 1* indicates a tubular element with solid walls, and *n = 2* indicates a tubular element with porous walls. The lattice relative density and length to radius ratio (for n greater than 0) are held constant and equal to 10^{-3} and 50 respectively.

Figures 16-19 show that structural hierarchy can substantially increase the strength of zero-expansion lattices. The strength enhancement is most pronounced for low density lattices.

Both tubular rib structure (order $n = 1$) and porous tubular ribs (order $n = 2$) greatly improve the resistance of lattice ribs to Euler buckling. The failure mode with the lowest stress

will govern the overall failure. So, if structural hierarchy gives rise to an Euler stress greater than stress associated with rib yield, then yielding will be the failure mode. Even so, overall stress (strength) is enhanced.

Conclusion

Structural hierarchy in lattices with tubular ribs enables zero expansion combined with enhanced ratio of strength to density. Zero expansion lattices with oriented porosity are achievable with positive CTE constituents including Invar-steel, Invar-brass, and Invar-aluminum, by way of tunable anisotropy. The interface between the nested constituents can be bonded or press-fit, more practicable than slip interfaces used in prior designs.

Structural hierarchy in lattices with curved bi-material ribs enables zero expansion combined with enhanced ratio of stiffness to density. The hierarchy enhances stiffness and strength because it entails thicker ribs of the same weight.

Acknowledgment

Support from DARPA-LLNL under the aegis of Judah Goldwasser is gratefully acknowledged.

References

1. Lakes R. Cellular solid structures with unbounded thermal expansion. *J. Mater. Sci. Lett.* 1996; 15: 475-477.

2. Lakes R. Cellular solids with tunable positive or negative thermal expansion of unbounded magnitude. *Appl. Phys. Lett.* 2007; 90: 221905. doi:10.1063/1.2743951

3. Lehman J, Lakes R. Stiff lattices with zero thermal expansion. *J. Intell. Mater. Syst. Struct.* 2012; 23(11): 1263-1268.

4. Lehman J, Lakes R. Stiff lattices with zero thermal expansion and enhanced stiffness via rib cross section optimization. *Int. J. Mech. Mater. Des.* 2013; Published online. doi: 10.1007/s10999-012-9210-x

5. Steeves CA, dos Santos e Lucato SL, He M, Antinucci E, Hutchinson JW, Evans AG. Concepts for structurally robust materials that combine low thermal expansion with high stiffness. *J. Mech. Phys. Solids* 2007; 55: 1803-1822.

6. Jefferson G, Parthasarathy TA, Kerans RJ. Tailorable thermal expansion hybrid structures. *Int. J. Solids Struct* 2009; 46: 2372-2387.

7. Lehman J, Lakes R. Stiff, strong zero thermal expansion lattices via the Poisson effect. *J. Mater. Res.* In Publication 2013.

8. Baird KM. Compensation for linear thermal expansion. *Metrologia* 1968; 4 (3): 145-146.

9. Baird KM. Thermal expansion compensation device. Patent No. 3528206. Canada. 1970, September 15.

10. Lakes R. Materials with structural hierarchy. *Nat.* 1993; 361: 511-515.

11. Woolger C. Invar nickel-iron alloy: 100 Years On. *Mater. World* 1996; 4 (6):332-333.

12. Agarwal BD, Broutman LJ. Analysis and performance of fiber composites. 2nd ed. New York: John Wiley and Sons, Inc; 1990.

13. ASM International Materials Properties Database Committee. ASM ready reference thermal properties of metals. Materials Park (Ohio): ASM International; 2002.

14. Cook RD, Young WC. Advanced mechanics of materials. 2nd ed. Upper Saddle River (New Jersey): Prentice-Hall Inc; 1999.

15. Beer FP, Johnston RE, DeWolf JT, Mazurek DF. Mechanics of materials. 5th ed. Boston: McGraw-Hill; 2009.

16. Deshpande V, Fleck NA, Ashby MF. Effective properties of the octet-truss lattice material. *J. Mech. Phys. Solids* 2001; 49: 1747-69.

17. Gibson LJ, Ashby MF. Cellular solids: structure and properties. 2nd ed. Cambridge (UK): Cambridge University Press; 1997.

18. Plastics Worldwide. Modern plastics encyclopedia. vol. 51 no. 10A. New York: McGraw-Hill Inc; 1974.